

THE VERY YOUNG TYPE IA SUPERNOVA 2013DY: DISCOVERY, AND STRONG CARBON ABSORPTION IN EARLY-TIME SPECTRA

WEIKANG ZHENG^{1,2}, JEFFREY M. SILVERMAN^{3,4}, ALEXEI V. FILIPPENKO¹, DANIEL KASEN^{5,6}, PETER E. NUGENT^{5,1}, MELISSA GRAHAM^{1,7,8}, XIAOFENG WANG⁹, STEFANO VALENTI^{7,8}, FABRIZIO CIABATTARI¹⁰, PATRICK L. KELLY¹, ORI D. FOX¹, ISAAC SHIVVERS¹, KELSEY I. CLUBB¹, S. BRADLEY CENKO¹¹, DAVE BALAM¹², D. ANDREW HOWELL^{7,8}, ERIC HSIAO¹³, WEIDONG LI^{1,14}, G. HOWIE MARION^{3,15}, DAVID SAND¹⁶, JOZSEF VINKO^{17,3}, J. CRAIG WHEELER³, AND JUJIA ZHANG^{18,19}

Draft version July 12, 2018

ABSTRACT

The Type Ia supernova (SN Ia) 2013dy in NGC 7250 ($d \approx 13.7$ Mpc) was discovered by the Lick Observatory Supernova Search. Combined with a predisccovery detection by the Italian Supernova Search Project, we are able to constrain the first-light time of SN 2013dy to be only 0.10 ± 0.05 d (2.4 ± 1.2 hr) before the first detection. This makes SN 2013dy the earliest known detection of an SN Ia. We infer an upper limit on the radius of the progenitor star of $R_0 \lesssim 0.25 R_\odot$, consistent with that of a white dwarf. The light curve exhibits a broken power law with exponents of 0.88 and then 1.80. A spectrum taken 1.63 d after first light reveals a C II absorption line comparable in strength to Si II. This is the strongest C II feature ever detected in a normal SN Ia, suggesting that the progenitor star had significant unburned material. The C II line in SN 2013dy weakens rapidly and is undetected in a spectrum 7 days later, indicating that C II is detectable for only a very short time in some SNe Ia. SN 2013dy reached a *B*-band maximum of $M_B = -18.72 \pm 0.03$ mag ~ 17.7 d after first light.

Subject headings: supernovae: general — supernovae: individual (SN 2013dy)

1. INTRODUCTION

Type Ia supernovae (SNe Ia) are used as calibratable candles with many important applications, including measurements of the expansion rate of the Universe (Riess et al. 1998; Perlmutter et al. 1999). However, the understanding of their progenitor systems and explosion mechanisms remains substantially incomplete. It is thought that SNe Ia are the product of the thermonuclear

explosions of C/O white dwarfs (Hoyle & Fowler 1960; Colgate & McKee 1969; see Hillebrandt & Niemeyer 2000 for a review), but very early discovery and detailed follow-up observations are essential for learning about the nature of the progenitor evolution and the nature of the explosion process. Recent examples of well-studied SNe Ia include SN 2009ig (Foley et al. 2012), SN 2011fe (Nugent et al. 2011; Li et al. 2011), and SN 2012cg (Silverman et al. 2012a); like SN 2013dy, they were discovered shortly after exploding.

Early discovery and identification give us the opportunity to obtain spectra when the SNe are still very young, yielding more insight into the composition of the SN blastwave (especially the outer layers) and its progenitor star. For example, while O is often seen (can be from both unburned material and a product of C burning), spectroscopic C is much more rare. In particular, strong C features have been seen only in a few “super-Chandrasekhar mass” SNe Ia: SNLS-03D3bb (SN 2003fg; Howell et al. 2006), SN 2006gz (Hicken et al. 2007), SN 2007if (Scalzo et al. 2010), and SN 2009dc (Yamanaka et al. 2009; Silverman et al. 2011; Taubenberger et al. 2011). Though often detectable in normal SNe Ia, C lines are usually not strong (e.g., Patat et al. 1996; Garavini et al. 2005; Nugent et al. 2011; Silverman et al. 2012b).

Here we present our observations and analysis of SN 2013dy, detected merely 0.10 d after first light. An early spectrum (1.63 d) exhibits an unusually strong absorption feature ~ 245 Å redder than Si II $\lambda 6355$, very likely produced by C II.

2. DISCOVERY AND OBSERVATIONS

The field of NGC 7250 has been observed by the 0.76 m Katzman Automatic Imaging Telescope (KAIT) more than 600 times over the past 15 yr as part of the Lick Observatory Supernova Search (LOSS; Filippenko et al.

arXiv:1310.5188v1 [astro-ph.CO] 19 Oct 2013

¹ Department of Astronomy, University of California, Berkeley, CA 94720-3411, USA.

² e-mail: zwk@astro.berkeley.edu .

³ Department of Astronomy, University of Texas, Austin, TX 78712, USA.

⁴ NSF Astronomy and Astrophysics Postdoctoral Fellow.

⁵ Lawrence Berkeley National Laboratory, Berkeley, California 94720, USA.

⁶ Department of Physics, University of California, Berkeley, 94720, USA.

⁷ Las Cumbres Observatory Global Telescope Network, 6740 Cortona Drive, Suite 102, Santa Barbara, CA 93117, USA.

⁸ Department of Physics, Broida Hall, University of California, Santa Barbara, CA 93106, USA.

⁹ Department of Physics, Tsinghua University, Beijing 100084, China.

¹⁰ Monte Agiale Observatory, Borgo a Mozzano, Lucca, 55023 Italy.

¹¹ Astrophysics Science Division, NASA Goddard Space Flight Center, Mail Code 661, Greenbelt, MD 20771, USA.

¹² Dominion Astrophysical Observatory, National Research Council of Canada.

¹³ Carnegie Observatories, Las Campanas Observatory, Colina El Pino, Casilla 601, Chile.

¹⁴ Deceased 2011 December 11.

¹⁵ Harvard-Smithsonian Center for Astrophysics, 60 Garden St., Cambridge, MA 02138, USA.

¹⁶ Physics Department, Texas Tech University, Lubbock, TX 79409, USA.

¹⁷ Department of Optics and Quantum Electronics, University of Szeged, Dóm tér 9, 6720 Szeged, Hungary.

¹⁸ Yunnan Astronomical Observatory, Chinese Academy of Sciences, 650011, Yunnan, China.

¹⁹ Key Laboratory for the Structure and Evolution of Celestial Objects, Chinese Academy of Sciences, Kunming 650011, China.

2001). In early 2011, the LOSS search strategy was modified to monitor fewer galaxies at a more rapid cadence with the objective of promptly identifying very young SNe (hours to days after explosion). The new software autonomously prompts KAIT to obtain a sequence of U , B , V , and unfiltered (roughly R) images when a new transient is discovered, usually only minutes after the discovery images were taken. One of the first successful discoveries using this technique was SN 2012cg (Silverman et al. 2012a), followed by several others (e.g., SN 2013ab, Blanchard et al. 2013; SN 2013dh, Kumar et al. 2013). Although multi-band follow-up photometry was not autonomously triggered for SN 2013dy on the night of discovery, it was triggered two days later. The trigger was not activated the first night because the SN was quite faint and multiple other (spurious) candidates were found in the discovery image. However, the autonomous trigger activated by the second KAIT image demonstrates that the software triggering capability functions well.

SN 2013dy was discovered (Casper et al. 2013) in an 18 s unfiltered KAIT image taken at 10:55:30 on 2013 July 10 (UT dates are used throughout) at $R = 17.19 \pm 0.05$ mag. We measure its J2000.0 coordinates to be $\alpha = 22^{\text{h}}18^{\text{m}}17^{\text{s}}.603$, $\delta = +40^{\circ}34'09''.54$, with an uncertainty of $0''.15$ in each coordinate. Figure 1 shows KAIT and the Sloan Digital Sky Survey (SDSS) finding chart near the SN location. SN 2013dy is $2''.3$ west and $26''.4$ north of the nucleus of the host galaxy NGC 7250, at a distance of 13.7 ± 3.0 Mpc (calculated from the Tully-Fisher relation; Tully et al. 2009), which gives the SN a projected distance of ~ 1.76 kpc from the nucleus. We note that there is a bright, blue region about $8''.7$ west and $6''.4$ south of the SN (projected distance ~ 0.71 kpc), which may be a star-forming region or merger (LEDA 214816; Paturel et al. 2000). It has been recently reported that the observed differences among SNe Ia may be tied to their birthplace environments (e.g., Kelly et al. 2010; Wang et al. 2013). However, it is unclear whether SN 2013dy has any connection with this star-forming region.

We obtained KAIT multi-band images almost every night for the following ~ 3 weeks, and they were reduced using our image-reduction pipeline (Ganeshalingam et al. 2010). Point-spread function photometry was then obtained using DAOPHOT (Stetson 1987) from the IDL Astronomy User’s Library²⁰. The SN instrumental magnitudes are calibrated to local SDSS standards transformed into the Landolt system²¹. We applied an image-subtraction procedure to remove host-galaxy light from only the unfiltered images, because multi-band images without the SN are not yet available. However, KAIT has a relatively small pixel scale ($0''.78$ pixel⁻¹), and the host background is quite uniform and faint in the KAIT images, so we believe that the contribution from the host galaxy is minor in all bands, especially considering the brightness of the SN. Comparisons of the subtracted and not subtracted unfiltered images yield nearly identical results (differences of ~ 0.1 mag or less).

Interestingly, an unfiltered prediscovery detection of

SN 2013dy was obtained at 02:04:11 July 10 (Casper et al. 2013) with the 0.5 m reflector at Monte Agliale Observatory as part of the Italian Supernova Search Project (ISSP). Additional confirmation images were taken on July 11 and 26. We have reprocessed the original images as part of this study. Owing to the relatively large pixel scale ($2''.32$ pixel⁻¹), the SN is blended with host-galaxy light. Using a template image taken on 2011 August 4, we performed the same subtraction method as for the KAIT unfiltered images. We then obtained photometry with an aperture of radius 1.5 pixels, a reasonable size given the seeing and large pixel scale.

Additional multi-band photometry in Johnson-Cousins $BVRI$ was obtained with the Las Cumbres Observatory Global Telescope (LCOGT) network of robotic 1.0 m telescopes (Brown et al. 2013). The LCOGT instrumental magnitudes are calibrated to local SDSS standards, transformed to $BVRJ$ ²².

Optical spectra of SN 2013dy were obtained on 8 different nights with DEIMOS (Faber et al. 2003) on the Keck II telescope (1.63 d), the 1.82 m Plaskett Telescope

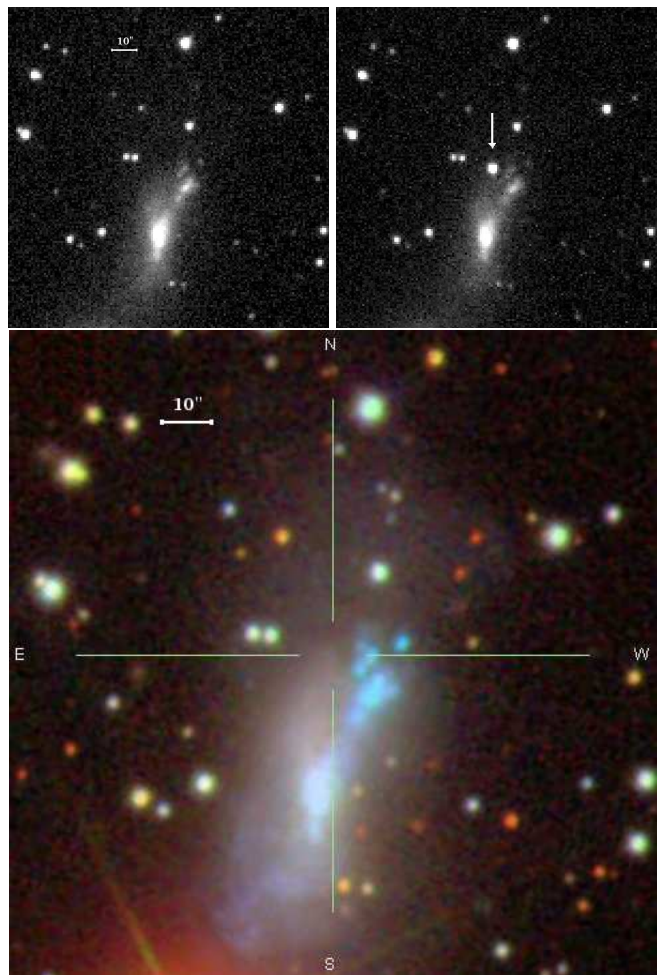


FIG. 1.— Top left: KAIT unfiltered template image. Top right: KAIT unfiltered image with the SN indicated by the arrow. Bottom: SDSS color composite of the field around SN 2013dy (position marked with crosshairs); the nucleus of NGC 7250 is to the south ($26''.5$ away), and a blue star-forming region is to the southwest ($\sim 10''.7$ away).

²⁰ <http://idlastro.gsfc.nasa.gov/>.

²¹ <http://www.sdss.org/dr7/algorithms/sdssUBVRITransform.html#Lupton2005>.

²² <http://www.sdss.org/dr7/algorithms/sdssUBVRITransform.html#Jester2005>.

of the National Research Council of Canada (3.30 d), YFOSC on the 2.4 m telescope at LiJiang Gaomeigu Station of YNAO (4.76 d), the Kast double spectrograph (Miller & Stone 1993) on the Shane 3 m telescope at Lick Observatory (5.43 d), the FLOYDS robotic spectrograph (Sand et al., in prep.) on the LCOGT 2.0 m Faulkes Telescope North on Haleakala, Hawaii (7.50, 8.57, 10.57 d), and the Marcario Low-Resolution Spectrograph (LRS; Hill et al. 1998) on the 9.2 m Hobby-Eberly Telescope (HET) at McDonald Observatory (11.27 d). Data were reduced following standard techniques for CCD processing and spectrum extraction using IRAF. The spectra were flux calibrated through observations of appropriate spectrophotometric standard stars.

3. ANALYSIS AND RESULTS

3.1. Light Curves

Figure 2 shows our *BVRI* and unfiltered light curves of SN 2013dy. Applying a low-order polynomial fit, we find that SN 2013dy reached a *B*-band peak magnitude of 13.28 ± 0.03 on 2013 July 27.71 ± 0.30 , ~ 17.7 d after first light. Assuming $E(B - V)_{\text{MW}} = 0.15$ mag (Schlegel et al. 1998), $E(B - V)_{\text{host}} = 0.15$ mag (see below), and $d = 13.7$ Mpc (Tully et al. 2009), this implies $M_B = -18.72 \pm 0.03$ (statistical only) mag, which is ~ 0.5 mag dimmer than the typical SN Ia, but still within the range of a “normal” SN Ia. The unfiltered band reached a peak of 12.81 ± 0.03 mag, which means our first detection of the SN from the ISSP image (18.71 mag, with a limiting magnitude of ~ 19.5) was taken when the SN was at only $\sim 0.43\%$ of its peak brightness.

In order to determine the time of first light²³, one can assume that the SN luminosity scales as the surface area of the expanding fireball, and therefore increases quadratically with time ($L \propto t^2$, commonly known as the t^2 model; Arnett 1982; Riess et al. 1999; Nugent et al. 2011). We restrict our model fit to the unfiltered data, which have the best phase coverage. Although ISSP images are also unfiltered, there might be possible differences between the KAIT and ISSP effective bandpasses. Fortunately, the second and third ISSP observations are between KAIT observations, and the ISSP magnitudes are consistent with the KAIT light curve, suggesting that the ISSP unfiltered band is very close to that of KAIT. Moreover, we measured isolated reference stars in the ISSP images and compared their magnitudes with the same stars in the KAIT images, finding consistent results between the two telescopes with differences < 0.04 mag. Thus, it is reasonable to combine the ISSP and KAIT unfiltered results.

Regardless, we first apply the fit only to KAIT fluxes in the first few days (before July 18). We find that a t^2 model cannot fit the data very well. We therefore free the exponent of the power law and obtain a best-fit value of 2.24 ± 0.08 , with a corresponding first-light time of -2.14 ± 0.17 d (relative to the first detection time, July 10.086). The exponent is about 3σ away from the t^2 model (marginally consistent). However, as can be

seen from the residual plot in Figure 2, the first night of KAIT data is below the fit, indicating an even faster light curve. This becomes more drastic if we include the first ISSP detection, which is far below the extrapolation of the $t^{2.24}$ fit. Thus, we refit the fluxes including both ISSP and KAIT data, but restricted to data taken before July 14. We find the best-fit power law exponent for these early data to be 1.15 ± 0.04 , with a corresponding first-light time of -0.31 ± 0.05 d. Note that the nondetection from KAIT on July 8.47 (limiting magnitude ~ 19.4) is consistent with both the $t^{1.15}$ fit and the $t^{2.24}$ fit.

The apparent change of the power law indices indicates a varying power law of the early rising light curve. Hence, we adopt a broken power law function, also widely used for fitting GRB afterglows (e.g., Zheng et al. 2012):

$$f = \left(\frac{t - t_0}{t_b} \right)^{\alpha_1} \left[1 + \left(\frac{t - t_0}{t_b} \right)^{s(\alpha_1 - \alpha_2)} \right]^{-1/s}, \quad (1)$$

where f is the flux, t_0 is the first-light time, t_b is the break time, α_1 and α_2 are the two power law indices before and after the break, and s is a smoothing parameter. The final fit result gives $t_0 = -0.10 \pm 0.05$ d, namely July 9.99, and $t_b = 3.14 \pm 0.30$ d, $s = -6.32 \pm 3.26$, $\alpha_1 = 0.88 \pm 0.07$, and $\alpha_2 = 1.80 \pm 0.10$, as shown in Figure 3.

With an estimated first-light time of -0.10 d (2.4 hr), this is the earliest detection of any SNe Ia, even earlier than for SN 2011fe (detected only 11.0 hr after first light; Nugent et al. 2011) and SN 2009ig (detected 17 hr after

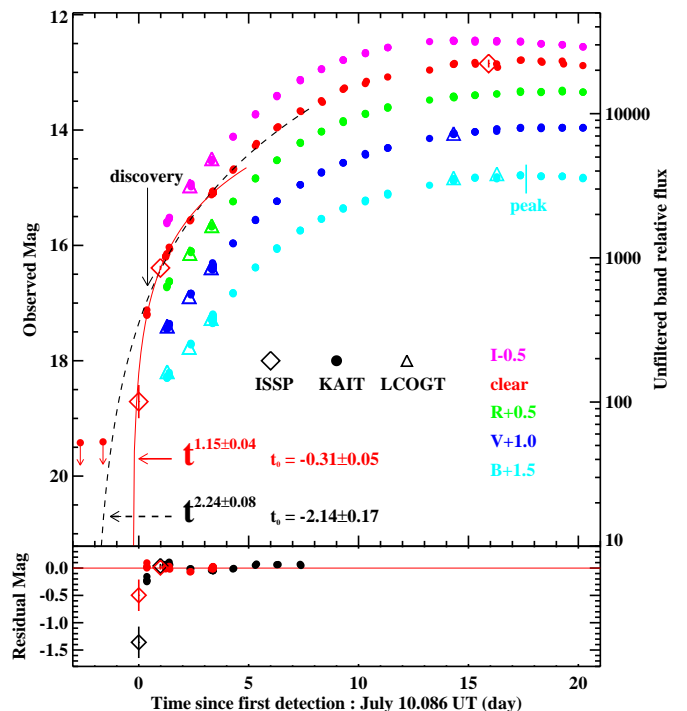


FIG. 2.— Multi-band light curves of SN 2013dy (top panel). Statistical errors are smaller than data points if not shown, and include any subtraction error. The solid red line is the $t^{1.15}$ fit for combined KAIT and ISSP unfiltered fluxes before July 14 (with an inferred first-light time of -0.31 d), while the dashed black line is the $t^{2.24}$ fit only for KAIT data before July 18 (with an inferred first-light time of -2.14 d). The residuals are shown in the bottom panel with the same color. This result indicates a varying (broken) power law of the early rising light curve, which we adopt; see Figure 3.

²³ Throughout this paper, we refer to the time of first light instead of explosion time, since the SN may exhibit a “dark phase” which can last for a few hours to days, between the moment of explosion and the first observed light (e.g., Rabinak, Livne, & Waxman 2012; Piro & Nakar 2012, 2013).

first light; Foley et al. 2012). It also makes SN 2013dy a rare case with more than one detection within the initial day after first light: there are 3 epochs of detection within 1 d and 5 epochs within 1.5 d.

Our best-fit broken power law model of the early light curve yields the following conclusions. (1) The t^2 model is not sufficient for every SN Ia; some SNe may have different power law exponents describing their rise (see also Piro & Nakar 2012). (2) The rising exponent may vary with time. Perhaps the usual t^2 model works well for previous SNe Ia because those examples did not have more than one observation to constrain the power law exponent within the first day. The varying exponent indicates that the very early fireball may exhibit significant changes in either the photospheric temperature, the velocity, or the fireball input energy during expansion. These changes may happen on a time scale of 2–4 d after first light. The very early light curve before the break time may be the contribution from the shock-heated cooling emission after shock breakout, which has a predicted

rising index of 1.5 ($f \propto t^{1.5}$; see Eq. 3 in Piro & Nakar 2013). However, our observed power law index is 0.88, smaller than predicted. The rising index also depends on underlying physical parameters; detailed analysis will be presented elsewhere.

Alternatively, the early-time observations constrain the emission from the ejecta, which can be used to limit the radius of the progenitor star as well as interaction with the circumstellar medium or a companion star (Kasen 2010). For SN 2013dy, the early ISSP unfiltered observation of ~ 17.89 mag (corrected for extinction) at 0.10 d limits any emission from this process to be $\nu L_\nu \lesssim 2.6 \times 10^{40}$ erg s $^{-1}$ at optical wavelengths. Comparing these parameters with those of SN 2011fe, which has a constraint on its progenitor star $R_0 \lesssim 0.1 R_\odot$ (see Fig. 4 of Nugent et al. 2011), our constraint for SN 2013dy is slightly weaker (factor of ~ 2.6), and so we infer the radius of the progenitor star to be $R_0 \lesssim 0.25 R_\odot$. Even if we conservatively assume the first-light time to be earlier, the same time as the KAIT upper limit (July 8.47), we can still find that $R_0 \lesssim 0.35 R_\odot$, consistent with a white dwarf progenitor.

3.2. Spectra

Figure 4 shows our spectra of SN 2013dy from the first ~ 2 weeks. Most exhibit narrow Na I D absorption from both the host galaxy and the Milky Way. The median redshift determined from these features is $z = 0.00383 \pm 0.00025$, consistent with the redshift given in SIMBAD (0.00389).

The equivalent width (EW) of Na I D absorption is often converted into reddening, but with large scatter over the empirical relationship (Poznanski et al. 2011). The median EW of Na I D from the host galaxy is measured to be $\sim 0.53 \text{ \AA}$, which yields a range of possible reddening values around $E(B - V)_{\text{host}} = 0.15$ mag (Poznanski et al. 2011). For Milky Way extinction, the measured median EW of Na I D is $\sim 0.50 \text{ \AA}$, corresponding to $E(B - V)_{\text{MW}} = 0.14$ mag, consistent with the value of $E(B - V)_{\text{MW}} = 0.15$ mag given by Schlegel et al. (1998); here we adopt the latter.

3.2.1. Species and Individual Lines

To help identify the species present in our spectra of SN 2013dy, we used the spectrum-synthesis code SYNAPPS (Thomas et al. 2011). A few examples of our fits are shown in Figure 4. Our first spectrum of SN 2013dy (1.63 d after first light) consists of absorption features from ions usually seen in SNe Ia (Ca II, Si II, Fe II, S II, and O I, as well as strong C II). All of these species have expansion velocities $\gtrsim 15,000$ km s $^{-1}$, similar to what was found in the earliest spectra of SN 2011fe (Parent et al. 2012). Figure 5 shows our measurements of individual line velocities (see Silverman et al. 2012c for details).

In addition to the usual photospheric absorption component of the Ca II near-infrared triplet, SN 2013dy exhibits a high-velocity feature (HVF) in our early spectra having a velocity of $\sim 26,000$ km s $^{-1}$. Similar absorption is also seen in a few other well-observed SNe, including SN 2005cf (Wang et al. 2009) and SN 2012fr (e.g., Maund et al. 2013; Childress et al. 2013). This HVF appears to be detached from the rest of the photosphere, slowing down to $\sim 23,000$ km s $^{-1}$ after three days (measured

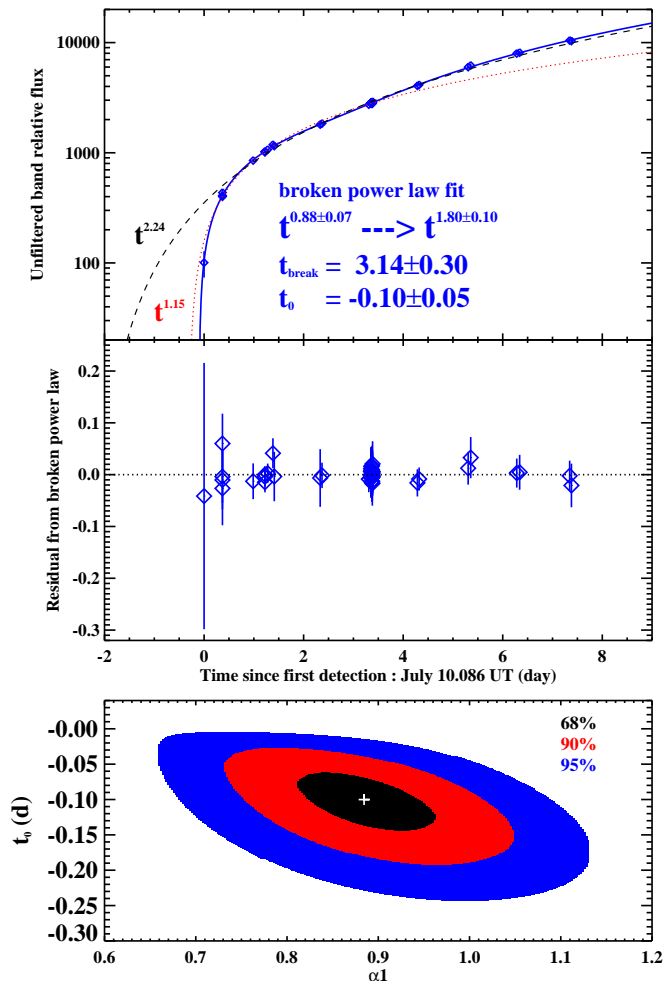


FIG. 3.— Top: the broken power law fit (solid blue) to the early unfiltered light curve, with the residuals shown in the middle panel. Compared with the two single power law results, the broken power law clearly improves the fit; the power law index changes from 0.88 to 1.80, with a break time of 3.14 d and a first-light time of -0.10 d; see text for details. Bottom: map of the χ^2 hypersurface around the minimum-fit result of t_0 and α_1 . The outbound for each color of black, red, and blue corresponds to 68%, 90%, and 95% confidence intervals (from inside to outside), respectively.

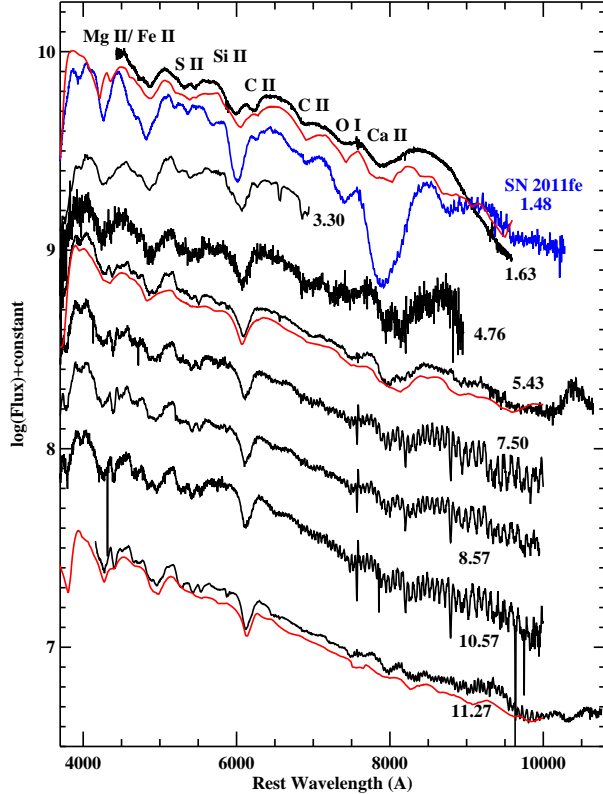


FIG. 4.— Spectra of SN 2013dy and a few SYNAPPS fits (red), along with comparison to the young SN 2011fe (blue). Each spectrum is labeled with its age relative to first light. Some major spectral features are labeled at the top. Wiggles redward of ~ 7500 Å in some of the spectra are produced by CCD fringing.

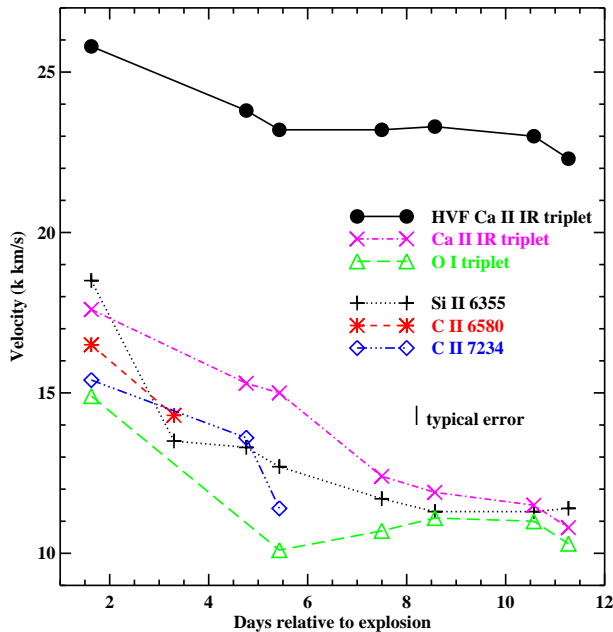


FIG. 5.— Expansion-velocity evolution of different lines measured from the spectra of SN 2013dy. Uncertainties are ~ 300 km s $^{-1}$, and are comparable to the size of the data points.

from the first spectrum) and maintaining that velocity through at least 11 d. As for Si II $\lambda 6355$, the velocity continuously slow down from $\sim 18,500$ km s $^{-1}$ at 1.63 d to $\sim 11,400$ km s $^{-1}$ at 11.27 d.

Interestingly, our first spectrum exhibits a strong line ~ 245 Å redward of the usual prominent Si II $\lambda 6355$. It is very likely to be the C II $\lambda 6580$ line; a weaker C II $\lambda 7234$ feature is also visible. Such strong C II lines are not usually seen in normal SNe Ia (Silverman et al. 2012b), but similar features have been observed in a few super-Chandrasekhar mass examples. Though C II is distinguishably detected in over 1/4 of all normal SNe Ia (e.g., Parrent et al. 2011; Silverman et al. 2012b), it is usually not very strong. However, spectra of other SNe Ia have generally not been obtained as early as our spectra of SN 2013dy. In fact, the C II $\lambda 6580$ line weakens rapidly in SN 2013dy; it became much weaker by 3.30 d, and it is undetectable after an age of ~ 1 week. Thus, the early discovery of SNe Ia and timely spectroscopic observations are crucial for detecting the C II features and studying their evolution.

The velocity of C II $\lambda 7234$ is slightly lower than that of C II $\lambda 6580$ in the 1.63 d spectrum, and both are also a bit below that of the photospheric component of Si II $\lambda 6355$, as seen in previous work (e.g., Silverman et al. 2012b). But after ~ 3 d, their velocities are similar to each other. The presence of C II with velocity comparable to that of Si II gives direct evidence that there exists some amount of unburned material. Moreover, the presence of both O I (often seen in normal SNe Ia) and C II suggests that the progenitor is probably a C+O white dwarf, consistent with the analysis of our early-time light curve.

3.2.2. Classification

Using the SuperNova IDentification code (SNID; Blondin & Tonry 2007), we find that SN 2013dy is spectroscopically similar to several normal SNe Ia, though some of our early spectra (7.50, 8.57, 10.57 d) also resemble those of the peculiar SN 1999aa and similar events (e.g., Li et al. 2001). Since the peak *B*-band brightness lies in the range of typical SN Ia luminosities, SN 2013dy is probably a normal SN Ia.

4. CONCLUSIONS

In this *Letter* we present optical photometry and spectroscopy of the Type Ia SN 2013dy, the earliest detection of an SN Ia thus far. The rising light curve shows a variable power-law exponent and its early-time spectrum exhibits a strong C II feature, both of which are not seen in previous studies of normal SNe Ia. Such well-studied objects will help us understand the underlying nature of SNe Ia.

A.V.F.'s group (and KAIT) at UC Berkeley have received financial assistance from the TABASGO Foundation, the Sylvia & Jim Katzman Foundation, the Christopher R. Redlich Fund, and NSF grant AST-1211916. J.M.S. is supported by an NSF postdoctoral fellowship under award AST-1302771. X. Wang acknowledges NNSFC grants 11073013 and 11178003, the Foundation of Tsinghua University (2011Z02170), and the Major State Basic Research Development Program (2013CB834903). J.V. is grateful for Hungarian OTKA

grant NN 107637. J.C.W. acknowledge support from NSF AST-1109801. This research used resources of NERSC, supported by DoE under Contract DE-AC02-05CH11231. Some data were obtained at the W. M. Keck Observatory, which was made possible by the gen-

erous financial support of the W. M. Keck Foundation. We thank the staffs of the various observatories at which data were obtained. We thank the anonymous referee for the useful suggestions that improved the paper.

REFERENCES

- Arnett, W. D. 1982, *ApJ*, 253, 785
 Blanchard, P., Zheng, W., Cenko, S. B., Li, W., et al. 2013, *CBET*, 3422
 Blondin, S., & Tonry, J. L. 2007, *ApJ*, 666, 1024
 Brown, T. M., et al. 2013, arXiv:1305.2437
 Casper, C., Zheng, W., Li, W., Filippenko, A. V., & Cenko, S. B., 2013, *CBET*, 3588
 Childress, M., et al. 2013, *ApJ*, 770, 29
 Colgate, S. A., & McKee, C. 1969, *ApJ*, 157, 623
 Faber, S. M., et al. 2003, *SPIE*, 4841, 1657
 Filippenko, A. V., Li, W. D., Treffers, R. R., & Modjaz, M. 2001, in *Small-Telescope Astronomy on Global Scales.*, ed. B. Paczyński, W. P. Chen, & C. Lemme (San Francisco: ASP), 121
 Foley, R. J., et al. 2012, *ApJ*, 744, 38
 Ganeshalingam, M., et al. 2010, *ApJS*, 190, 418
 Garavini, G., et al. 2005, *AJ*, 130, 2278
 Hicken, M., et al. 2007, *ApJ*, 669, L17
 Hill, G. J., et al. 1998, *SPIE*, 3355, 375
 Hillebrandt, W., & Niemeyer, J. C. 2000, *ARA&A*, 38, 191
 Howell, D. A., et al. 2006, *Nature*, 443, 308
 Hoyle, F., & Fowler, W. A. 1960, *ApJ*, 132, 565
 Kasen, D. 2010, *ApJ*, 708, 1025
 Kelly, P. L., et al. 2010, *ApJ*, 715, 743
 Kumar, S., Fuller, K., Zheng, W., et al. 2013, *CBET*, 3561
 Li, W., Filippenko, A. V., Treffers, R. R., Riess, A. G., Hu, J., & Qiu, Y. 2001, *ApJ*, 546, 734
 Li, W., et al. 2011, *Nature*, 480, 348
 Maund, J. R., et al. 2013, *MNRAS*, 433, L20
 Miller, J. S., & Stone, R. P. S. 1993, *Lick Obs. Tech. Rep. 66* (Santa Cruz: Lick Obs.)
 Nugent, P. E., et al. 2011, *Nature*, 480, 344
 Parrent, J. T., et al. 2011, *ApJ*, 732, 30
 Parrent, J. T., et al. 2012, *ApJ*, 752, 26
 Patat, F., Benetti, S., Cappellaro, E., et al. 1996, *MNRAS*, 278, 111
 Paturel, G., et al. 2000, *A&AS*, 144, 475
 Perlmutter, S., et al. 1999, *ApJ*, 517, 565
 Piro, A., & Nakar, E. 2012, arXiv:1211.6438
 Piro, A., & Nakar, E. 2013, *ApJ*, 769, 67
 Poznanski, D., Ganeshalingam, M., Silverman, J. M., & Filippenko, A. V. 2011, *MNRAS*, 415, L81
 Rabinak, I., Livne, E. & Waxman, E. 2012, *ApJ*, 757
 Riess, A. G., et al. 1998, *AJ*, 116, 1009
 Riess, A. G., Filippenko, A. V., Li, W., & Schmidt, B. P. 1999, *AJ*, 118, 2668
 Scalzo, R. A., et al. 2010, *ApJ*, 713, 1073
 Schlegel, D. J., Finkbeiner, D. P., & Davis, M. 1998, *ApJ*, 500, 525
 Silverman, J. M., et al. 2011, *MNRAS*, 410, 585
 Silverman, J. M., et al. 2012a, *ApJ*, 756, L7
 Silverman, J. M., et al. 2012b, *MNRAS*, 425, 1917
 Silverman, J. M., et al. 2012c, *MNRAS*, 425, 1819
 Stetson, P. B. 1987, *PASP*, 99, 191
 Taubenberger, S., et al. 2011, *MNRAS*, 412, 2735
 Thomas, R. C., Nugent, P. E., & Meza, J. C. 2011, *PASP*, 123, 237
 Tully, R., et al., 2009, *AJ*, 138, 323
 Wang, X., et al. 2009, *ApJ*, 697, 380
 Wang, X., et al. 2013, *Science*, 340, 170
 Yamanaka, M., et al. 2009, *ApJ*, 707, L118
 Zheng, W., et al. 2012, *ApJ*, 751, 90